

Journal of Mechanics of Materials and Structures

**ANALYSIS OF HARD COATINGS ON A SUBSTRATE CONTAINING
INHOMOGENEITIES**

Kun Zhou, Leon M. Keer and Q. Jane Wang

Volume 6, No. 1-4

January–June 2011

 **mathematical sciences publishers**

ANALYSIS OF HARD COATINGS ON A SUBSTRATE CONTAINING INHOMOGENEITIES

KUN ZHOU, LEON M. KEER AND Q. JANE WANG

We investigate the effect stiff inhomogeneities in the substrate beneath a hard coating have on the elastic field. The solution of multiple interacting three-dimensional inhomogeneities in a half-space is utilized by modeling a coating layer as an inhomogeneity of finite size. The study shows that stiff inhomogeneities in the substrate do not worsen the cracking and debonding of hard coatings, but are still detrimental to the yielding behavior of the substrate even though it is under the protection of a hard coating.

1. Introduction

Inhomogeneities with elastic moduli different from those of their surrounding matrix are ubiquitous in solid materials, and their presence significantly affects the physical and mechanical properties of materials at the local and the global scale [Mortensen 2007]. For a given matrix material, inhomogeneities are categorized into two types: stiff ones which have larger Young's modulus than the matrix and compliant ones with smaller Young's modulus. Generally, stiff inhomogeneities can cause stress to increase in the matrix material, compared with compliant inhomogeneities. Nonmetallic inhomogeneities such as oxides and nitrides are typical stiff inhomogeneities in steels.

Hard coatings have been used to protect substrate matrix materials from wear and yielding damage; however, they are subject to interfacial cracking and debonding and surface cracking failure under combined heavy normal and tangential loading. Such failure may be more likely when inhomogeneities in the substrate are closer to the interface of the coating-substrate system. To improve reliability and functionality, it would be useful to understand how and to what extent inhomogeneities degrade the performance of coatings. However, almost no theoretical or experimental studies on such problems exist, due to the complex nature of the solution for the elastic field of inhomogeneities in a coating-substrate system. Such a solution would be a foundation for further studies but is not yet available.

Eshelby [1957] pioneered the work on inhomogeneities by solving the elastic field of an ellipsoidal inhomogeneity embedded in an infinite matrix with the equivalent inclusion method (EIM). The EIM assumes that an inhomogeneity can be modeled by a homogenous inclusion with unknown equivalent eigenstrain to be determined. A homogeneous inclusion has the same material properties as the matrix but contains eigenstrain, a generic term that refers to inelastic strain such as plastic strain, misfit strain, thermal expansion and phase transformation [Mura 1987]. Since then, the EIM has been used extensively to investigate a single inhomogeneity [Johnson et al. 1980a; 1980b; Nakasone et al. 2000; Dong et al. 2002; Kirilyuk and Levchuk 2005], two interacting inhomogeneities [Moschovidis and Mura 1975; Fond

Keywords: hard coating, inhomogeneity, equivalent inclusion method, yielding.

et al. 2001; Shodja and Sarvestani 2001; Shodja et al. 2003], and multiple inhomogeneities [Nemat-Nasser et al. 1982; 1993; Luo and Weng 1987; Hori and Nemat-Nasser 1993; Shodja and Roumi 2005; Duan et al. 2006] in an infinite matrix. However, the interactions of all inhomogeneities were not fully taken into account in the referred studies of multiple inhomogeneities. Other methods have also been used to study a single or two inhomogeneities in an infinite matrix, e.g., the complex function method [Kushch et al. 2005], the boundary element method [Tan et al. 1992], and the volume integral equation method [Dong et al. 2003].

So far, few investigations have been conducted on inhomogeneities in a half-space. These studies include a circular rigid disc [Hunter and Gamblen 1974; Selvadurai 2001], an ellipsoidal inhomogeneity [Tsuchida and Mura 1983], a hemispheroidal inhomogeneity [Kouris and Mura 1989], a spheroidal inhomogeneity [Tsuchida et al. 2000], two concentric spherical inhomogeneities [Molchanov et al. 2002], and one or multiple two-dimensional arbitrarily shaped inhomogeneities [Kuo 2007; 2008]. The boundary element method was used in these last two works, while the Papkovitch–Neuber or the Boussinesq displacement potential was used to solve the problems in the other referred works. Studies were also performed on a single or multiple inhomogeneities in one of two joining half-surfaces of dissimilar materials, e.g., [Meguid and Zhu 1995; Yu and Kuang 2003; Brusselaars et al. 2007]. The results of those studies can be applicable to the problems of inhomogeneities in a half-space when one of the two joining half-spaces is set free.

Recently, Zhou et al. [2010] solved multiple interacting three-dimensional inhomogeneities of arbitrary shape in a half-space using the EIM. In this paper, we apply this solution to study the effect of inhomogeneities embedded in the substrate of a coating-substrate system on the elastic field of the coating by modeling the coating as an inhomogeneity with respect to the substrate.

2. Methodology

Consider a coating-substrate system that contains multiple inhomogeneities in the substrate and is subject to external loading on the surface of the coating. The loading is prescribed as a known function and assumed to be located within a circular area of radius R . The solution strategy is to model the coating by a cuboidal inhomogeneity of size $L_x \times L_y \times H$ with H equal to the thickness of the coating. The dimensions L_x and L_y are set to be much larger than both R and H to simulate the infinite dimensions of the coating in the x - y plane. In this way, the original coating-substrate problem with inhomogeneities is converted into a half-space problem with inhomogeneities.

Let us now turn to a half-space with elastic moduli C_{ijkl} ($i, j, k, l = 1, 2, 3$) that contains n inhomogeneities Ω_ψ ($\psi = 1, 2, \dots, n$) with elastic moduli C_{ijkl}^ψ . Since there is no inelastic strain within Ω_ψ , the total strain ε_{ij} at any point within Ω_ψ is the elastic strain ε_{ij}^e . According to Hooke's law, the stress σ_{ij} within Ω_ψ is given by $\sigma_{ij} = C_{ijkl}^\psi \varepsilon_{kl}$. Using the EIM, each Ω_ψ is simulated by a homogeneous inclusion Ω_ψ^I that has the same elastic moduli as the matrix but contains equivalent eigenstrain ε_{ij}^* to be determined. The equivalent eigenstrains ε_{ij}^* are introduced to represent material differences of the inhomogeneities, the interactions among them, and their responses to the external load (applied stresses). The total strain ε_{ij} within Ω_ψ^I contains elastic strain ε_{ij}^e and equivalent eigenstrain ε_{ij}^* , and according to Hooke's law, the stress σ_{ij} within Ω_ψ^I is given by $\sigma_{ij} = C_{ijkl}(\varepsilon_{kl} - \varepsilon_{kl}^*)$. Furthermore, σ_{ij} can be decomposed into $\sigma_{ij} = \sigma_{ij}^* + \sigma_{ij}^0$, where σ_{ij}^* is the eigenstress caused by the equivalent eigenstrains ε_{ij}^* in all Ω_ψ^I and σ_{ij}^0

the applied stress due to the external load. From these three stress expressions, the governing equation is established as

$$C_{ijkl}^{\Psi} C_{klmq}^{-1} \sigma_{mq}^* - \sigma_{ij}^* + C_{ijkl}^{\Psi} \varepsilon_{kl}^* = \sigma_{ij}^0 - C_{ijkl}^{\Psi} C_{klmq}^{-1} \sigma_{mq}^0 \quad (\psi = 1, 2, \dots, n; i, j, k, l, m, q = 1, 2, 3). \quad (1)$$

where the equivalent eigenstrains ε_{ij}^* are unknowns. This equation cannot be solved until the relationship between σ_{ij}^* and ε_{ij}^* is determined.

Figure 1 illustrates a cuboidal computational domain D of size $L_x \times L_y \times L_z$ that contains n inhomogeneities Ω_{ψ} in a half-space, which is bounded by the surface plane $z = 0$ in the x - y - z coordinate system. The cuboidal inhomogeneity Ω_1 of size $L_x \times L_y \times H$ at the surface is used to model a layer of coating of thickness H . The domain D is discretized into $N_x \times N_y \times N_z$ small cuboidal elements of the same size, and each Ω_{ψ} is then geometrically approximated by a collection of such cuboidal elements. The finer the discretization, the more accurate the approximation would be. If the size of the cuboidal element is small enough, each cuboidal inhomogeneity within Ω_{ψ} can be treated as containing uniform eigenstrain. It is noted that the eigenstrain within Ω_{ψ} is still nonuniform. For convenience, each cuboidal element is indexed by a sequence of three integers $[\alpha, \beta, \gamma]$ ($0 \leq \alpha \leq N_x - 1$, $0 \leq \beta \leq N_y - 1$, $0 \leq \gamma \leq N_z - 1$). Using the EIM, each cuboidal inhomogeneity is simulated as a cuboidal homogenous inclusion with uniform equivalent eigenstrain. Thus, (1) can be recast into

$$\begin{aligned} (\mathbf{C}_{\alpha,\beta,\gamma} \mathbf{C}^{-1} - \mathbf{I}) \boldsymbol{\sigma}_{\alpha,\beta,\gamma}^* + \mathbf{C}_{\alpha,\beta,\gamma} \boldsymbol{\varepsilon}_{\alpha,\beta,\gamma}^* &= (\mathbf{I} - \mathbf{C}_{\alpha,\beta,\gamma} \mathbf{C}^{-1}) \boldsymbol{\sigma}_{\alpha,\beta,\gamma}^0, \\ (\mathbf{C}_{\alpha,\beta,\gamma} \in \mathbf{C}_{\psi} \quad (\psi = 1, 2, \dots, n), \quad 0 \leq \alpha \leq N_x - 1, \quad 0 \leq \beta \leq N_y - 1, \quad 0 \leq \gamma \leq N_z - 1), \end{aligned} \quad (2)$$

where \mathbf{C} , $\boldsymbol{\varepsilon}^*$, $\boldsymbol{\sigma}^*$ and $\boldsymbol{\sigma}^0$ are written in matrix form and \mathbf{I} is a unit matrix. The symbol \mathbf{C} denotes the elastic moduli of the substrate matrix, $\mathbf{C}_{\alpha,\beta,\gamma}$ denotes the elastic moduli of the cuboid $[\alpha, \beta, \gamma]$ within Ω_{ψ} , $\boldsymbol{\varepsilon}_{\alpha,\beta,\gamma}^*$ the uniform equivalent eigenstrain within $[\alpha, \beta, \gamma]$, $\boldsymbol{\sigma}_{\alpha,\beta,\gamma}^*$ the stress at an observation point inside $[\alpha, \beta, \gamma]$ caused by the equivalent eigenstrains in all the cuboidal inclusions, and $\boldsymbol{\sigma}_{\alpha,\beta,\gamma}^0$ the applied stress at the observation point. All the observation points are chosen to be at the center of each cuboid.

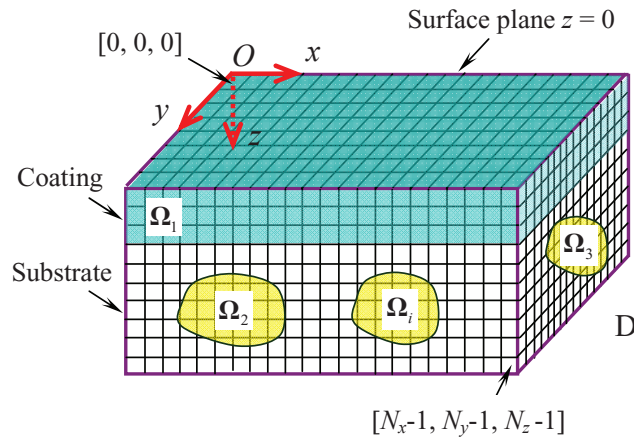


Figure 1. Discretization of a computational domain D into $N_x \times N_y \times N_z$ cuboids. The domain D contains n arbitrarily shaped inhomogeneities in an isotropic half-space, where Ω_1 is used to model a layer of coating on the substrate matrix.

The final solvable form for (2) is given in [Zhou et al. 2010] as

$$(\mathbf{C}_{\alpha,\beta,\gamma}\mathbf{C}^{-1} - \mathbf{I}) \sum_{\phi=0}^{N_z-1} \sum_{\zeta=0}^{N_y-1} \sum_{\xi=0}^{N_x-1} \mathbf{A}_{\alpha-\xi,\beta-\zeta,\gamma-\phi} \boldsymbol{\varepsilon}_{\xi,\zeta,\phi}^* + \mathbf{C}_{\alpha,\beta,\gamma} \boldsymbol{\varepsilon}_{\alpha,\beta,\gamma}^* = (\mathbf{I} - \mathbf{C}_{\alpha,\beta,\gamma}\mathbf{C}^{-1}) \boldsymbol{\sigma}_{\alpha,\beta,\gamma}^0$$

$$(\mathbf{C}_{\alpha,\beta,\gamma} \in \mathbf{C}_\psi (\psi = 1, 2, \dots, n), 0 \leq \alpha \leq N_x - 1, 0 \leq \beta \leq N_y - 1, 0 \leq \gamma \leq N_z - 1). \quad (3)$$

where $\mathbf{A}_{\alpha-\xi,\beta-\zeta,\gamma-\phi}$ relates the eigenstress $\boldsymbol{\sigma}_{\alpha,\beta,\gamma}^*$ at the observation point in the cuboid $[\alpha, \beta, \gamma]$ to the uniform eigenstrain $\boldsymbol{\varepsilon}_{\xi,\zeta,\phi}^*$ in the cuboid $[\xi, \zeta, \phi]$. The expression for $\mathbf{A}_{\alpha-\xi,\beta-\zeta,\gamma-\phi}$ is given in the paper by Chiu [1978] who solved the elastic field of a cuboid containing uniform eigenstrain in a half-space. Chiu's solution shows that there are stress singularities at certain edges and corners of the cuboid, depending upon the types of eigenstrain in the cuboid (also see [Chiu 1977; Mura 1987]). Nevertheless, the stress singularities would not affect the solution of (3) because the observation points where the stresses are concerned are taken only at the center of each cuboid.

Equation (3) can be solved by the conjugated gradient method [Shewchuk 1994], a well-established method for solving linear equations by iteration. Furthermore, the fast Fourier transform technique can be used for rapid calculation of the summations in (3) to achieve computational efficiency [Zhou et al. 2009]. Once all the eigenstrains $\boldsymbol{\varepsilon}^*$ are determined, the eigenstress $\boldsymbol{\sigma}^*$ due to $\boldsymbol{\varepsilon}^*$ is known and then the overall stress field $\boldsymbol{\sigma}$ is obtained by $\boldsymbol{\sigma} = \boldsymbol{\sigma}^* + \boldsymbol{\sigma}^0$.

3. Results and discussion

The study is performed on the elastic analysis of a layer of WC hard coating on a steel substrate in which a stiff cuboidal Al_2O_3 inhomogeneity is formed near the substrate surface prior to coating deposition, as illustrated in Figure 2. The steel matrix has Young's modulus $E = 210$ GPa and Poisson's ratio $\nu = 0.28$,

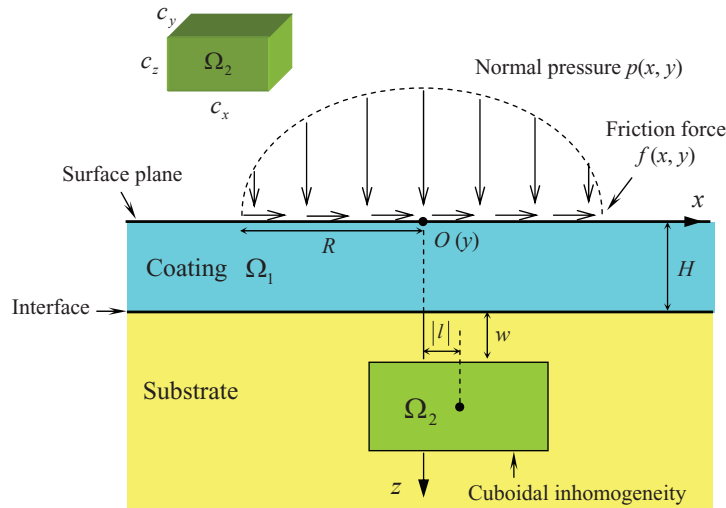


Figure 2. Schematic of a cuboidal inhomogeneity located beneath the interface of a coating-substrate system. The surface of the coating is subject to pressure and friction force.

the WC coating has $E_1 = 670$ GPa and $\nu_1 = 0.28$, and the Al_2O_3 inhomogeneity has $E_2 = 344$ GPa and $\nu_2 = 0.25$. The coating surface, bounded by the plane $z = 0$ in the x - y - z Cartesian coordinate system, is subjected to the prescribed normal pressure $p(x, y) = p_0(1 - (x/R)^2 - (y/R)^2)^{1/2}$ and friction force $f(x, y) = \mu p(x, y)$ in a circle of radius R . The coating thickness is denoted by H , and the cases of $h \leq 0.5R$ are mainly investigated. The cuboidal inhomogeneity has dimensions $c_x = c_y = R$ and $c_z = 0.5R$; its depth from the interface is denoted by w . The center of the cuboid is located in the plane $y = 0$ and distanced from the plane $x = 0$ by $|l|$ with l being the x -coordinate value of the center.

In the calculation, a computational domain of size $16R \times 16R \times 1.5R$ is used and the coating is simulated by the cuboidal inhomogeneity Ω_1 of $16R \times 16R \times H$. The cuboid Ω_1 has much larger dimension in the length and width directions than in the thickness direction in order to approximate the effect of infinite dimensions that the coating has in the x - y plane. The dimension $16R$ is also much larger than the radius R of the pressure area on the coating surface. The inhomogeneity, as mentioned, may have singularities at its edges and corners, but these singularities would not affect the stress calculation.

The case of $H = 0.5R$, $w = 0.25R$, $l = 0$, and $\mu = 0.3$ is first studied and shows that both the surface and interfacial stresses of the coating approach zero approximately at $x = \pm 4R$. Therefore, it is justifiable to model the infinitely extended coating by an inhomogeneity of finite size embedded at $x = \pm 8R$. Figure 3 presents the surface stress component σ_x^{surf} and the interfacial stress components σ_x^{int} , σ_z^{int} and σ_{xz}^{int} within the coating in the central plane $y = 0$ and along the x direction. All the stress components are normalized by the peak pressure p_0 at $(0, 0, 0)$. Results show that the surface normal stress σ_x^{surf} is tensile in the area behind the friction direction ($x < -R$), but compressive both in the pressure area and in the area ahead of the friction direction ($x > -R$). The stress σ_x^{surf} reaches its maximum tensile value around the edge of the pressure area at $x = -R$, and therefore is likely to cause crack nucleation there. The interfacial normal stress σ_x^{int} within the coating is tensile in the area under the surface pressure and its maximum value is comparable to that of σ_x^{surf} . This tensile stress may cause cracks to nucleate at the interface and then grow into the film along the direction perpendicular to the interface or cause the kinking of

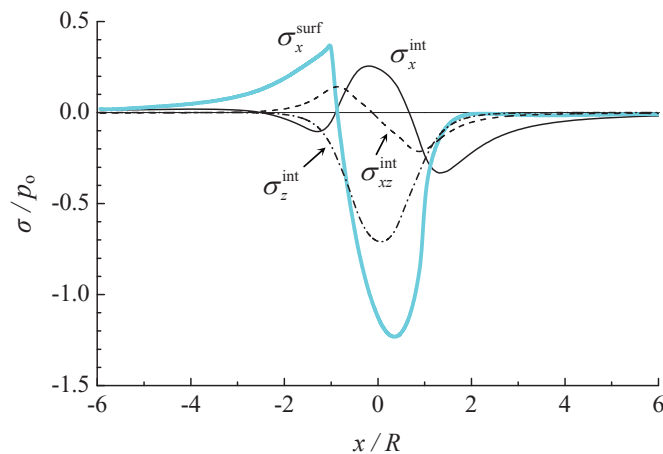


Figure 3. The component σ_x^{surf} of the surface stress and the components σ_x^{int} , σ_z^{int} , and σ_{xz}^{int} of the interfacial stress in the coating along the x -axis direction in the computational domain of size $16R \times 16R \times 1.5R$.

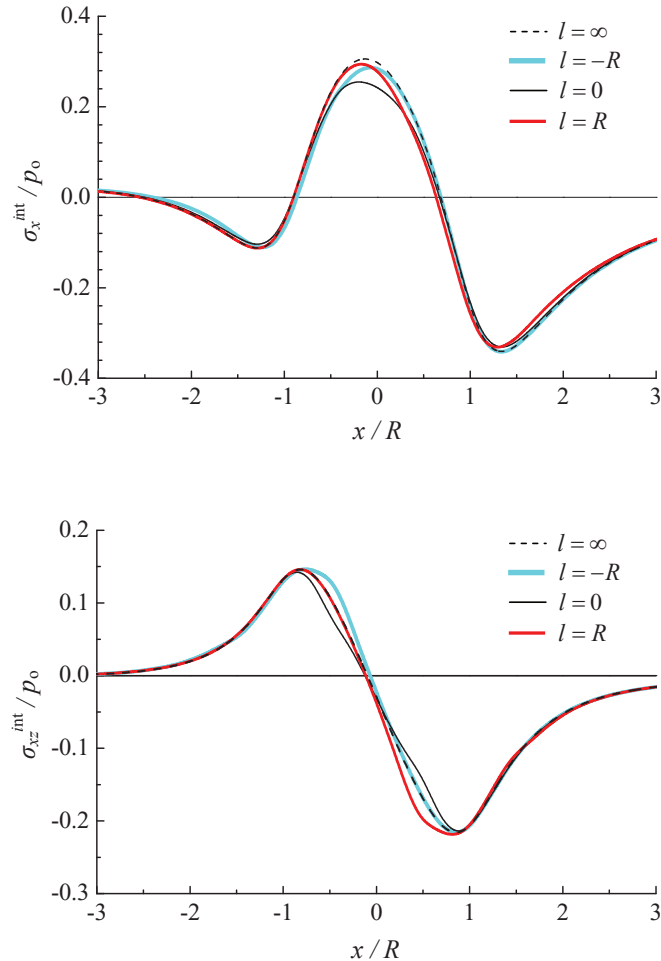


Figure 4. Effect of the horizontal position of the inhomogeneity Ω_2 on the interfacial normal stress σ_x^{int} (top) and shear stress σ_{xz}^{int} (bottom) within the coating.

interfacial cracks. Besides cracking within the coating, interfacial debonding of the coating is another damage phenomenon that needs to be considered. The interfacial shear stresses σ_{xz}^{int} affect the adhesion of the coating onto the substrate; their low magnitude would generally lead to good adhesion, thereby preventing the occurrence of interfacial debonding. Figure 3 shows that σ_{xz}^{int} reaches positive and negative maximum values in the locations approximately beneath the edges of surface pressure area ($x = \pm R$). It is predicted that interfacial debonding is likely to start at such locations.

We then study the effect of the inhomogeneity Ω_2 on cracking and debonding of the coating. Figure 4 compares the interfacial stress components σ_x^{int} and σ_{xz}^{int} among the cases for different horizontal locations of the inhomogeneity Ω_2 . The results show that the presence of Ω_2 decreases the tensile values of σ_x^{int} , compared with when Ω_2 is absent ($l = \infty$). The maximum tensile value of σ_x^{int} is decreased by about 17% when Ω_2 is directly beneath the peak surface pressure ($l = 0$). The decrease becomes smaller when Ω_2 is horizontally displaced from $l = 0$ to $l = -R$ or $l = R$. On the other hand, the change in both the

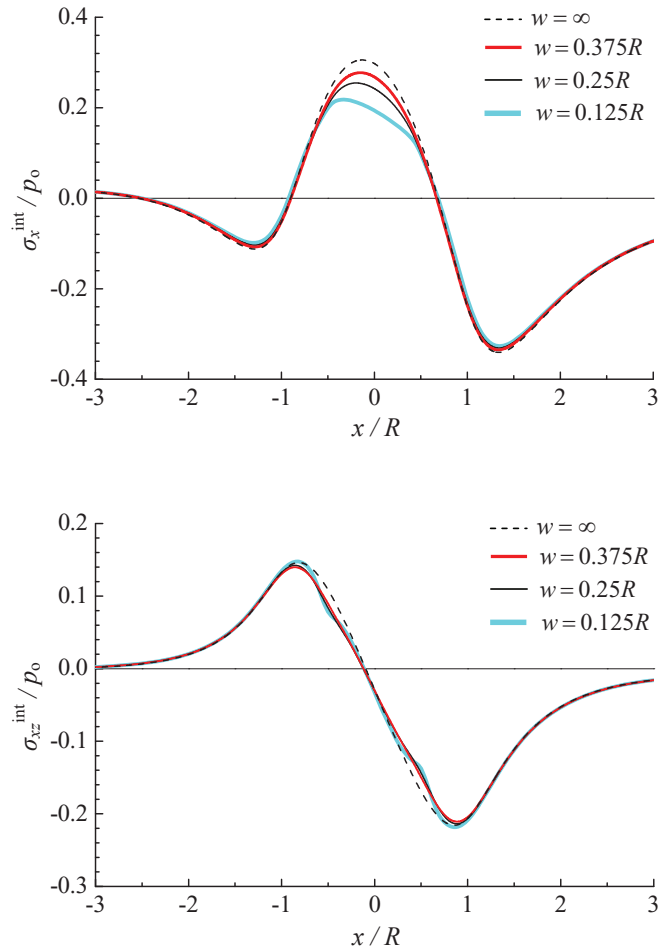


Figure 5. Effect of the depths of the inhomogeneity Ω_2 on the interfacial normal stress σ_x^{int} (top) and shear stress σ_{xz}^{int} (bottom) within the coating.

maximum positive and negative magnitudes of σ_{xz}^{int} is almost inappreciable. At $l = 0$, σ_{xz}^{int} decreases in the areas near the points of maximum negative and positive magnitudes, while at $l = -R$ ($l = R$), σ_{xz}^{int} increases in the area near the point of the maximum positive (negative) magnitude. Nevertheless, the overall change in σ_{xz}^{int} is not significant.

Figure 5 compares the interfacial stress components σ_x^{int} and σ_{xz}^{int} among the cases for different depths of the inhomogeneity Ω_2 at $l = 0$ and shows that as Ω_2 approaches the interface, the maximum tensile value of σ_x^{int} decreases and the reduction reaches about 27% at the depth $w = 0.125R$. The overall change in σ_{xz}^{int} is not significant except that the peak and valley shapes of σ_{xz}^{int} are narrower in the presence of Ω_2 than in the absence of Ω_2 ($w = \infty$).

Figures 4 and 5 demonstrate that the presence of stiff inhomogeneities in the substrate would not worsen the cracking and debonding of a hard coating and instead may likely play a role to decrease the possibility of their occurrence.

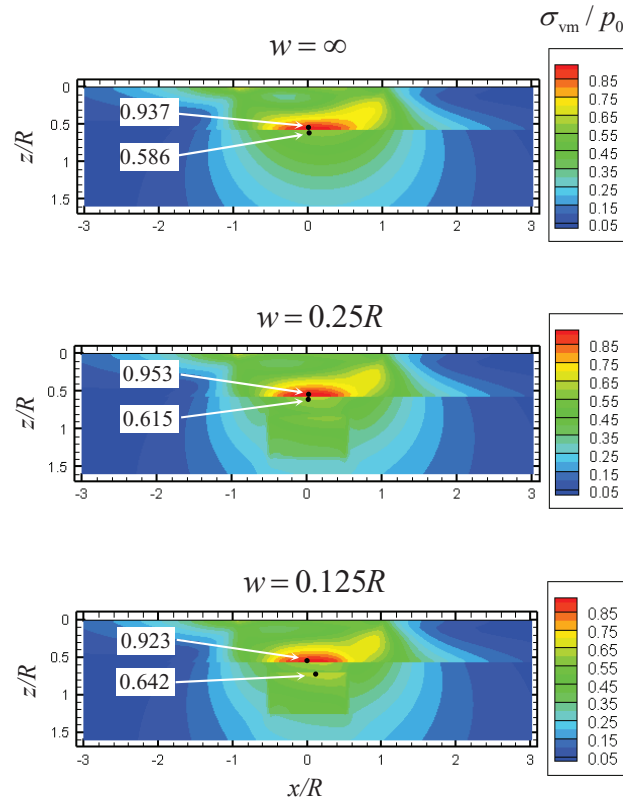


Figure 6. Effect of the depths of the inhomogeneity Ω_2 on the von Mises stress field in the coating-substrate system. The coating has a thickness of $0.5R$.

Figure 6 further presents the normalized von Mises stresses $\bar{\sigma}_{vm}$ in both the coating and the substrate for different depths of the inhomogeneity Ω_2 at $l = 0$. In the absence of Ω_2 ($w = \infty$), the maximum von Mises stress $\bar{\sigma}_{vm}^{\max}$ in the coating reaches 0.937 at the interface location approximately beneath the peak surface pressure. As Ω_2 approaches the interface, $\bar{\sigma}_{vm}^{\max}$ in the coating slightly increases to 0.953 and then decreases to 0.923, and its location remains the same. The increase in $\bar{\sigma}_{vm}^{\max}$ is almost negligible (about 1.7%). In contrast, $\bar{\sigma}_{vm}^{\max}$ in the substrate monotonically increases from 0.586 to 0.642, and its location changes from the interface location to the edge plane of the inhomogeneity Ω_2 . The increase in $\bar{\sigma}_{vm}^{\max}$ is significant (about 8.7%) and means yielding is more likely to occur in the substrate. Therefore, stiff inhomogeneities are still detrimental to the yielding behavior of the substrate even though it is protected by a layer of hard coating.

The thickness of a coating is a key parameter that affects its performance. The previous examples consider coatings of thickness $H = 0.5R$. The coatings with a thinner thickness $H = 0.25R$ are also studied. In Figure 7, the solid lines plot the surface stress component σ_x^{surf} and the interfacial stress components σ_x^{int} and σ_{xz}^{int} in the coating for the case of $H = 0.25R$, $w = 0.25R$, $l = 0$, and $\mu = 0.3$ along the x -axis, while the dashed lines represent the corresponding stress components for the case in the absence of the inhomogeneity Ω_2 . Their comparison shows that the presence of Ω_2 does not increase σ_x^{surf} , σ_x^{int} and σ_{xz}^{int} or cause significant change to them. Thus, for a thinner hard coating, it is still valid

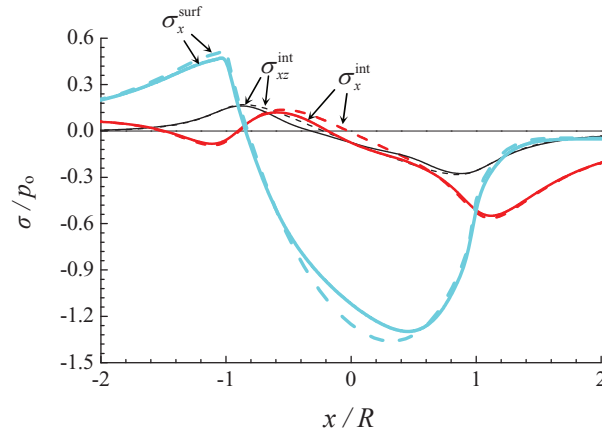


Figure 7. The surface stress component σ_x^{surf} and the interfacial stress components σ_x^{int} and σ_{xz}^{int} in the coating of thickness $H = 0.25R$ along the x -axis direction.

to draw the conclusion that stiff inhomogeneities in the substrate would not worsen the cracking and debonding of the coating.

Figure 7 shows that the maximum surface tensile stress σ_x^{surf} is much larger than the maximum interfacial tensile stress σ_x^{int} , which leads to the conclusion that surface cracking may start much earlier than cracking nucleated at the interface or dominate the damage mechanisms. An optimal design of hard coatings should balance the two cracking mechanisms to avoid the early occurrence of either one of them. The proper selection of coating thickness is a way to achieve this balance. Figure 3 demonstrates that when the coating is selected to have the thickness of $H = 0.5R$, the maximum tensile value of σ_x^{surf} is close to that of σ_x^{int} .

The normalized von Mises stresses $\bar{\sigma}_{\text{vm}}$ in both the coating and the substrate are presented in Figure 8 and show that as the inhomogeneity is located closer to the coating-substrate interface, $\bar{\sigma}_{\text{vm}}$ in the substrate increases and the increase reaches about 11%, which demonstrates again that detrimental effect of the stiff inhomogeneity on the yielding behavior of the substrate must be accounted for. Furthermore, the comparison between Figures 6 and 8 shows that a thicker coating ($X = 0.5R$) can provide better yielding protection to the substrate than a thinner coating ($H = 0.25R$).

Inhomogeneities can become stringers or clusters during their formation process. We investigate a stringer of Al_2O_3 inhomogeneities in the WC-coated steel substrate. The stringer is modeled as three identical cuboidal Al_2O_3 inhomogeneities, which have the same dimension as the previously studied single inhomogeneity and are equally distanced by $0.25R$. Figure 9 compares the von Mises stress field of the stringer between the two cases in which the coating has different thicknesses of $H = 0.5R$ and $h = 0.25R$. The stringer is located beneath the interface at the depth $w = 0.125R$ and shows that the interactions among the inhomogeneities distort the stress field around them and the distortion becomes stronger as the coating becomes thinner.

Although this study focuses on inhomogeneities of cuboidal shape, it should be noted that the present method is also capable of handling inhomogeneities of any arbitrary shapes. An arbitrarily shaped geometry can be approximated by the appropriate arrangement of multiple infinitesimal cuboidal elements.

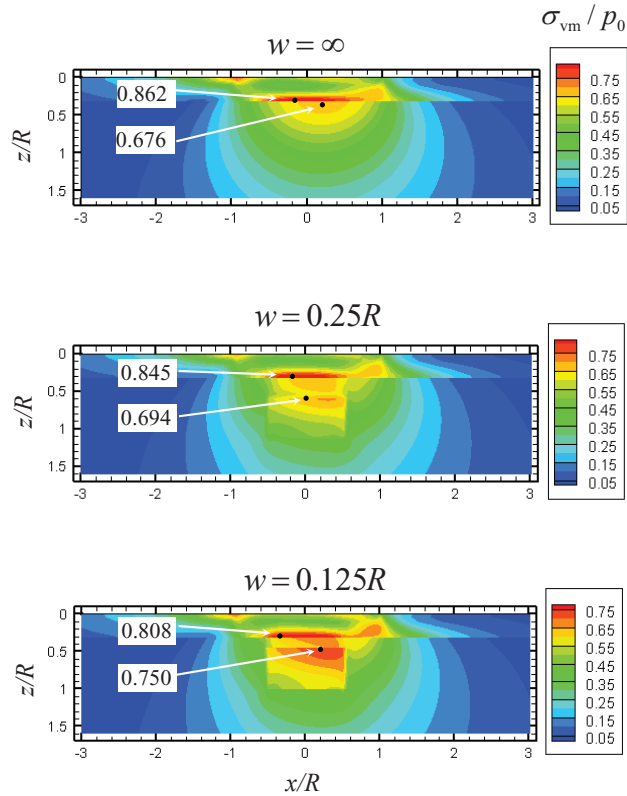


Figure 8. Effect of the depths of the inhomogeneity Ω_2 on the von Mises stress field in the coating-substrate system. The coating has a thickness of $0.25R$.

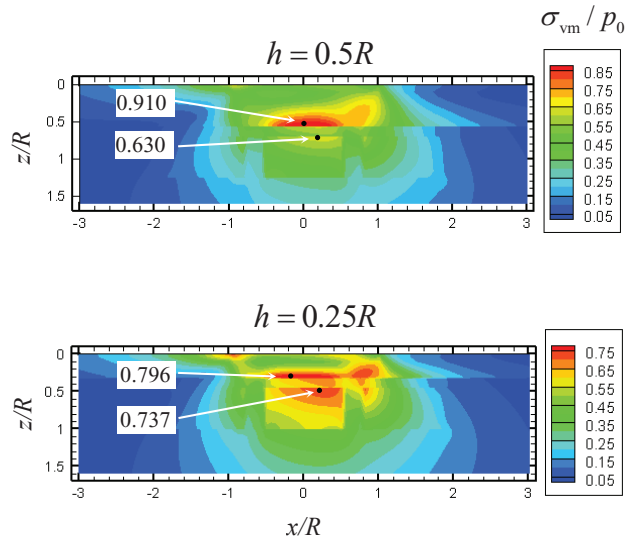


Figure 9. Effect of the depths of the inhomogeneity Ω_2 on the von Mises stress field in the coating-substrate system. The coating has a thickness of $0.25R$.

4. Conclusions

The effect of stiff inhomogeneities on the elastic field of hard coatings is studied by using the solution of multiple interacting three-dimensional inhomogeneities of arbitrary shape in a half-space. In the utilization of the inhomogeneity solution, a layer of coating is modeled by an inhomogeneity of finite size embedded in the half-space, which has much larger dimensions in the horizontal directions than in the depth direction to simulate the effect of the finitely extended dimensions of the coating. The study shows:

- (1) Stiff inhomogeneities formed in the substrate would not worsen the cracking and debonding of a hard coating.
- (2) Stiff inhomogeneities are still detrimental to the yielding behavior of the substrate even though coated by a layer of hard coating.

These considerations may provide guidance to minimize the potential damage induced by inhomogeneities to coating-substrate systems.

This study also suggests that the effect of inhomogeneities on yielding and plastic zone expansion cannot be neglected when a film-substrate system containing inhomogeneities is subject to elastic-plastic indentation. Based on the present method, a further study can be conducted to develop an elastic-plastic indentation model that takes into account inhomogeneities for indentation tests.

Acknowledgements

The authors would like to acknowledge the Timken Company, the United States Office of Naval Research, and the Center for Surface Engineering and Tribology at Northwestern University for financial support.

References

- [Brusselaars et al. 2007] N. Brusselaars, S. G. Mogilevskaya, and S. L. Crouch, "A semi-analytical solution for multiple circular inhomogeneities in one of two joined isotropic elastic half-planes", *Eng. Anal. Bound. Elem.* **31**:8 (2007), 692–705.
- [Chiu 1977] Y. P. Chiu, "On the stress field due to initial strains in a cuboid surrounded by an infinite elastic space", *J. Appl. Mech. (ASME)* **44**:4 (1977), 587–590.
- [Chiu 1978] Y. P. Chiu, "On the stress field and surface deformation in a half space with a cuboidal zone in which initial strains are uniform", *J. Appl. Mech. (ASME)* **45**:2 (1978), 302–306.
- [Dong et al. 2002] C. Y. Dong, Y. K. Cheung, and S. H. Lo, "A regularized domain integral formulation for inclusion problems of various shapes by equivalent inclusion method", *Comput. Methods Appl. Mech. Eng.* **191**:31 (2002), 3411–3421.
- [Dong et al. 2003] C. Y. Dong, S. H. Lo, and Y. K. Cheung, "Numerical solution of 3D elastostatic inclusion problems using the volume integral equation method", *Comput. Methods Appl. Mech. Eng.* **192**:1-2 (2003), 95–106.
- [Duan et al. 2006] H. L. Duan, Y. Jiao, X. Yi, Z. P. Huang, and J. Wang, "Solutions of inhomogeneity problems with graded shells and application to core-shell nanoparticles and composites", *J. Mech. Phys. Solids* **54**:7 (2006), 1401–1425.
- [Eshelby 1957] J. D. Eshelby, "The determination of the elastic field of an ellipsoidal inclusion, and related problems", *Proc. R. Soc. Lond. A* **241**:1226 (1957), 376–396.
- [Fond et al. 2001] C. Fond, A. Riccardi, R. Schirrer, and F. Montheillet, "Mechanical interaction between spherical inhomogeneities: an assessment of a method based on the equivalent inclusion", *Eur. J. Mech. A Solids* **20**:1 (2001), 59–75.
- [Hori and Nemat-Nasser 1993] M. Hori and S. Nemat-Nasser, "Double-inclusion model and overall moduli of multi-phase composites", *Mech. Mater.* **14**:3 (1993), 189–206.

- [Hunter and Gamblen 1974] S. C. Hunter and D. Gamblen, "The theory of a rigid circular disc ground anchor buried in an elastic soil either with adhesion or without adhesion", *J. Mech. Phys. Solids* **22**:5 (1974), 371–399.
- [Johnson et al. 1980a] W. C. Johnson, Y. Y. Earmme, and J. K. Lee, "Approximation of the strain field associated with an inhomogeneous precipitate, 1: Theory", *J. Appl. Mech. (ASME)* **47**:4 (1980), 775–780.
- [Johnson et al. 1980b] W. C. Johnson, Y. Y. Earmme, and J. K. Lee, "Approximation of the strain field associated with an inhomogeneous precipitate, 2: The cuboidal inhomogeneity", *J. Appl. Mech. (ASME)* **47**:4 (1980), 781–788.
- [Kirilyuk and Levchuk 2005] V. S. Kirilyuk and O. I. Levchuk, "Stress state of a transversely isotropic medium with an arbitrarily oriented spheroidal inclusion", *Prik. Mekh.* **41**:2 (2005), 33–40. In Russian; translated in *Int. Appl. Mech.* **41**:2 (2005), 137–143.
- [Kouris and Mura 1989] D. A. Kouris and T. Mura, "The elastic field of a hemispherical inhomogeneity at the free surface of an elastic half space", *J. Mech. Phys. Solids* **37**:3 (1989), 365–379.
- [Kuo 2007] C.-H. Kuo, "Stress disturbances caused by the inhomogeneity in an elastic half-space subjected to contact loading", *Int. J. Solids Struct.* **44**:3-4 (2007), 860–873.
- [Kuo 2008] C.-H. Kuo, "Contact stress analysis of an elastic half-plane containing multiple inclusions", *Int. J. Solids Struct.* **45**:16 (2008), 4562–4573.
- [Kushch et al. 2005] V. I. Kushch, S. V. Shmegeera, and V. A. Buryachenko, "Interacting elliptic inclusions by the method of complex potentials", *Int. J. Solids Struct.* **42**:20 (2005), 5491–5512.
- [Luo and Weng 1987] H. A. Luo and G. J. Weng, "On Eshelby's inclusion problem in a three-phase spherically concentric solid, and a modification of Mori–Tanaka's method", *Mech. Mater.* **6**:4 (1987), 347–361.
- [Meguid and Zhu 1995] S. A. Meguid and Z. H. Zhu, "Stress distribution in dissimilar materials containing inhomogeneities near the interface using a novel finite element", *Finite Elem. Anal. Des.* **20**:4 (1995), 283–298.
- [Molchanov et al. 2002] I. N. Molchanov, I. S. Levchenko, N. N. Fedonyuk, A. N. Khimich, and T. V. Chistyakova, "Numerical simulation of the stress concentration in an elastic half-space with a two-layer inclusion", *Prik. Mekh.* **38**:3 (2002), 65–71. In Russian; translated in *Int. Appl. Mech.* **38**:3 (2002), 308–314.
- [Mortensen 2007] A. Mortensen, *Concise encyclopedia of composite materials*, 2nd ed., Elsevier, Amsterdam, 2007.
- [Moschovidis and Mura 1975] Z. A. Moschovidis and T. Mura, "Two-ellipsoidal inhomogeneities by the equivalent inclusion method", *J. Appl. Mech. (ASME)* **42**:4 (1975), 847–852.
- [Mura 1987] T. Mura, *Micromechanics of defects in solids*, Martinus Nijhoff, The Hague, 1987.
- [Nakasone et al. 2000] Y. Nakasone, H. Nishiyama, and T. Nojiri, "Numerical equivalent inclusion method: a new computational method for analyzing stress fields in and around inclusions of various shapes", *Mater. Sci. Eng. A* **285**:1-2 (2000), 229–238.
- [Nemat-Nasser et al. 1982] S. Nemat-Nasser, T. Iwakuma, and M. Hejazi, "On composites with periodic structure", *Mech. Mater.* **1**:3 (1982), 239–267.
- [Nemat-Nasser et al. 1993] S. Nemat-Nasser, M. Yu, and M. Hori, "Solids with periodically distributed cracks", *Int. J. Solids Struct.* **30**:15 (1993), 2071–2095.
- [Selvadurai 2001] A. P. S. Selvadurai, "On the displacements of an elastic half-space containing a rigid inhomogeneity", *Int. J. Geomech. (ASCE)* **1**:2 (2001), 149–174.
- [Shewchuk 1994] J. R. Shewchuk, *An introduction to the conjugate gradient method without the agonizing pain*, Carnegie Mellon University, Pittsburgh, PA, 1994.
- [Shodja and Roumi 2005] H. M. Shodja and F. Roumi, "Overall behavior of composites with periodic multi-inhomogeneities", *Mech. Mater.* **37**:2-3 (2005), 343–353.
- [Shodja and Sarvestani 2001] H. M. Shodja and A. S. Sarvestani, "Elastic fields in double inhomogeneity by the equivalent inclusion method", *J. Appl. Mech. (ASME)* **68**:1 (2001), 3–10.
- [Shodja et al. 2003] H. M. Shodja, I. Z. Rad, and R. Soheilifard, "Interacting cracks and ellipsoidal inhomogeneities by the equivalent inclusion method", *J. Mech. Phys. Solids* **51**:5 (2003), 945–960.
- [Tan et al. 1992] C. L. Tan, Y. L. Gao, and F. F. Afagh, "Anisotropic stress analysis of inclusion problems using the boundary integral equation method", *J. Strain Anal. Eng. Des.* **27**:2 (1992), 67–76.

- [Tsuchida and Mura 1983] E. Tsuchida and T. Mura, "The stress field in an elastic half space having a spheroidal inhomogeneity under all-around tension parallel to the plane boundary", *J. Appl. Mech. (ASME)* **50**:4a (1983), 807–816.
- [Tsuchida et al. 2000] E. Tsuchida, Y. Arai, K. Nakazawa, and I. Jasiuk, "The elastic stress field in a half-space containing a prolate spheroidal inhomogeneity subject to pure shear eigenstrain", *Mater. Sci. Eng. A* **285**:1-2 (2000), 339–345.
- [Yu and Kuang 2003] J. H. Yu and Z. B. Kuang, "The stress analysis of an ellipsoidal inhomogeneity in dissimilar media", *Compos. Sci. Technol.* **63**:7 (2003), 955–966.
- [Zhou et al. 2009] K. Zhou, W. W. Chen, L. M. Keer, and Q. J. Wang, "A fast method for solving three-dimensional arbitrarily shaped inclusions in a half space", *Comput. Methods Appl. Mech. Eng.* **198**:9-12 (2009), 885–892.
- [Zhou et al. 2010] K. Zhou, L. M. Keer, Q. J. Wang, X. Ai, K. Sawamiphakdi, P. Glaws, and M. Paire, "Interactions of multiple arbitrarily-shaped 3D inhomogeneous inclusions in a half space", 2010. Submitted manuscript.

Received 21 Jun 2010. Revised 28 Oct 2010. Accepted 4 Nov 2010.

KUN ZHOU: kzhou@ntu.edu.sg

Department of Mechanical Engineering, Northwestern University, 2145 Sheridan Road, Evanston, IL 60208-3100, United States

Current address: School of Mechanical and Aerospace Engineering, Nanyang Technological University, 50 Nanyang Avenue, Singapore 639798, Singapore

LEON M. KEER: l-keer@northwestern.edu

Department of Mechanical Engineering, Northwestern University, 2145 Sheridan Road, Evanston, IL 60208-3100, United States

Q. JANE WANG: qwang@northwestern.edu

Department of Mechanical Engineering, Northwestern University, 2145 Sheridan Road, Evanston, IL 60208-3100, United States